

**STUDY OF REGIONAL BROADBAND WAVES FROM EARTHQUAKES AND MAN-INDUCED  
EVENTS IN NE CHINA**

Rong-Mao Zhou<sup>1</sup>, Brian W. Stump<sup>1</sup>, and Christopher T. Hayward<sup>1</sup>  
Zhi-Xian Yang<sup>2</sup>, and Yun-Tai Chen<sup>2</sup>

Southern Methodist University<sup>1</sup> and China Seismological Administration<sup>2</sup>

Sponsored by Air Force Research Laboratory

Contract No. DTRA01-02-C-0003

**ABSTRACT**

We investigate the use of intermediate period surface wave magnitude,  $M_s$ , and high-frequency body wave magnitude,  $m_b$ , from regional mining explosions for event discrimination using techniques originally intended for teleseismic observations but modified for regional application. The magnitudes,  $M_s$  and  $m_b$  were estimated for an event that occurred in an iron mine in China (QianAn Explosion) with explosive yield of 1.3 kiloton and were compared to similar estimates from four kiloton-size mining explosions in Wyoming, USA. These magnitude estimates for mining explosions were compared to values from previous studies that included earthquakes and contained, single-fired explosions (Stevens and Day, 1985; Bonner et al., 2003). Although the previous studies examined mostly larger events, the Wyoming and China mining events plot in or near the earthquake population. Data from an anomalous Wyoming event, a blast in which a failure of the timing system caused a large portion of the blast pattern to simultaneously detonate, plots within the explosion population with  $m_b$  4.4. The simultaneous detonation of a large portion of the blast array increased the body wave magnitude but had little effect on surface wave amplitudes. The actual values of  $M_s$  and  $m_b$  suggest that the surface waves generated by long-time-duration mining explosions can make them appear earthquake like. The data from the single anomalous shot indicates that if a significant part of the total explosives is simultaneously detonated the event will fall into the explosion population.

We continue data acquisition at 10 stations around the Beijing area and moved five stations into the Haicheng area, the second proposed study area. Following the Haicheng network installation, two local events occurred approximately 165 km southwest of the network with magnitude  $M_L$  2.8 and 3.3 on August 25, 2004. These data illustrate the value of low noise sites in conducting regional studies of moderate sized events.

Finally, the complementary nature of Chinese digital station data to our study is demonstrated by some selected events. Observations from the QianAn explosion illustrate the value of these permanent three-component stations to our network observations providing improved event location and source characterization.

## OBJECTIVES

The deployment of the broadband seismic network operated by the Southern Methodist University (SMU) and the Institute of Geophysics, China Earthquake Administration (IGCEA, formerly IGCSB) has been completed. The current operating network includes 10 stations around the Yanqing-Huailai Basin, NW of Beijing and five stations in the Haicheng, NE China (Figure 1). The seismic data has been archived into the IRIS DMC database. The goals of this collaborative study between SMU and IGCEA are to develop a database of earthquakes and man-induced events; to refine event locations in Yanqing-Huailai Basin and Haicheng area; to understand source characterization of natural and man-induced events; and to separate source and propagation path effects at regional distances.

Beijing and Haicheng are two regions of historical natural and man-induced seismicity as well as a seismic hazard. The region includes the site of the first successful earthquake prediction in 1975 near Haicheng and the great Tangshan earthquake in 1976. The broadband seismic network provides near-source and regional coverage for the study area. Data from this network has been used to constrain the preliminary velocity structure around Beijing (Zhou, 2004) and investigate event discrimination for mining explosions (Zhou et al., 2004).

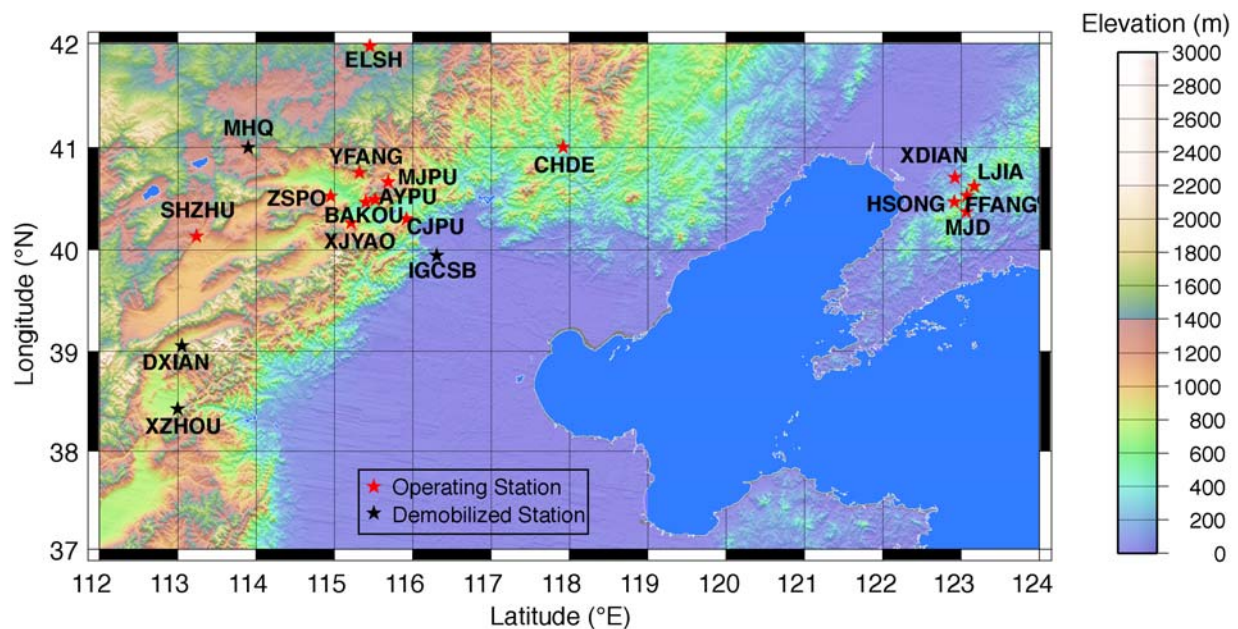


**Figure 1. Map of the SMU-IGPCEA Broadband Seismic Network (Operating stations: red stars; Demobilized stations: black stars).**

## RESEARCH ACCOMPLISHED

### The Completion of Deployment of the Broadband SMU-IGCEA Network

The deployment of the broadband SMU-IGCEA network was proposed in two phases. In Phase I, we deployed stations around the Yanqing-Huailai basin, and extended the network into the Haicheng area in Phase II. We continue data acquisition at 10 stations around the Beijing area. At the beginning of August, 2004, the group at IGCEA demobilized three stations at XZHOU, DXIAN and MHQ and installed five stations in Haicheng, Liaoning Province, the second proposed study area. The current SMU-IGCEA Broadband Seismic Network is summarized in Figure 1.

### Data Archive

Data is archived locally at each site. Periodic visits to the sites provide the opportunity to retrieve the data where it is stored on a Sun Ultra 10 at IGCSB, Beijing. Data is transferred to SMU by disk exchange. All data from Phase 1 has

been converted to SEED format and archived at the Data Manage Center at the Incorporated Research Institutions for Seismology (IRIS DMC). Data through September 2004 from Phase II were also been converted to SEED format and archived at IRIS DMC. The group at IGCEA has collected the data for September 2004 to May 2005 and will ship them to SMU. We are anticipating conversion and storage in July 2005.

### $M_s$ : $m_b$ Discriminant of Mining Explosions

Comparing  $M_s$  and  $m_b$  values for earthquakes and nuclear explosions has proven to be a successful teleseismic discriminant (Stevens and Day, 1985) since for a common body wave magnitude, earthquakes are more efficient than explosions in generating surface waves. The theoretical understanding of this relationship is related to the source function of the two event types, the materials surrounding the source, and the source depth.

$M_s$  in these teleseismic studies was defined for Rayleigh waves (Gutenberg, 1945) with periods near 20 s for events recorded at epicentral distances greater than  $20^\circ$ . Marshall and Basham (1972) suggested that  $M_s$  determination may be extended to smaller events and shorter periods with a path correction, which can be estimated from the quantification of dispersion curves for intermediate period surface waves. Application of such estimates to the explosion waveforms and the determination of regional body wave magnitudes provides for the investigation of such measures as discriminants between earthquakes and explosions.

We investigate the use of intermediate period surface wave magnitude,  $M_s$ , and high frequency body wave magnitude,  $m_b$ , from regional mining explosions for event discrimination. The magnitudes,  $M_s$  and  $m_b$  were estimated for the event occurred in an iron mine in China with explosive 1.3 kiloton and compared to the results of four kiloton-size mining explosions in Wyoming, USA (Zhou et al., 2004). For the events in Wyoming, we use the Denny et al. (1987) body wave magnitude formula which was specifically developed for the Western US from an extensive database of earthquakes and nuclear explosions at or near the Nevada Test Site. We use the formula for stable continent to estimate  $m_b$  for the QianAn event (Evernden, 1967).

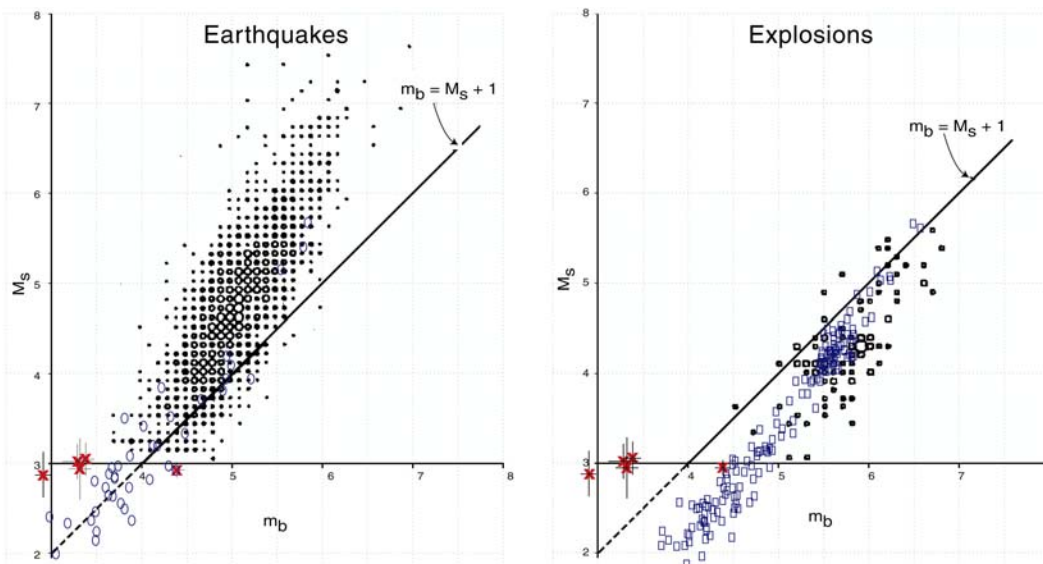


**Figure 2. The  $m_b$  :  $M_s$  plots for earthquakes (left) and explosions (right). Original figures are from Stevens and Day (1985) superposed with results from Bonner *et al.* 2003 (blue ellipses for earthquakes and blue rectangles for explosions) and our results (red x) with the standard deviations in gray.**

Figure 2 presents the  $M_s$  and  $m_b$  results from our study with the comparison to two previous studies that included earthquakes and contained single-fired explosions (Stevens and Day, 1985; Bonner et al., 2003) and examined mostly larger events than those in this study. All of our events fall at the very smallest magnitude range of the Stevens and Day study. Since the events are small, all of the estimates are based upon regional observations, whereas the Stevens and Day (1985) observations are primarily teleseismic. Despite these significant differences it is interesting to compare results. Except for the anomalous event (96214), all of our mining blasts plot in the

earthquake population, a result consistent with the robust intermediate period surface waves generated from these events.

The one anomalous event (96214) had about the same surface wave magnitude as the other events but the body wave magnitude is almost one full magnitude unit higher moving it into the explosion population. The only difference between this event and the other four is the time over which the explosion was detonated with a significant part of the explosive array being nearly simultaneously detonated.

Figure 3 presents the vertical component raw data for event 96214 recorded at PD31, a broadband seismic station of the permanent IMS array PDAR, and the filtered seismograms with frequency bandwidth of 0.0625 ~ 0.25 Hz, and 1.0 ~ 16.0 Hz. The spectral composition of event 95236, a single-fired explosion (22,700 kg) detonated at the same mine on 24 Aug., 1995 (Stump et al., 2003) and the normal production shot event 96201 are also presented in Figure 3. Figure 3(d) shows that the waveform characteristics of this anomalous event at high frequency (1 ~ 16 Hz) matches those from the single-fired explosion. In addition, the comparison illustrates that the cast shots generate intermediate surface waves and the single-fire explosion does not. The simultaneous detonation of a large portion of blast array increased the body wave magnitude but had little effect on surface wave amplitudes. The actual values of  $M_s$  and  $m_b$  suggest that the surface waves generated by long duration mining explosions can make them appear earthquake like. The data from a single anomalous shot indicates that if a significant part of the total explosives is simultaneously detonated the event will fall into the explosion population.

The source duration was estimated from the design delay times in the explosions as 4.4, 3.2, 3.6 and 5.6 s for 96201, 96214, 96215 and 97226, respectively. Zhou and Stump (2004) illustrated the source duration contribution to the fundamental Rayleigh wave in their Figure 20. This comparison here also suggests that the time function of mining and single-fired explosion may play a critical role in the performance of this discriminant.

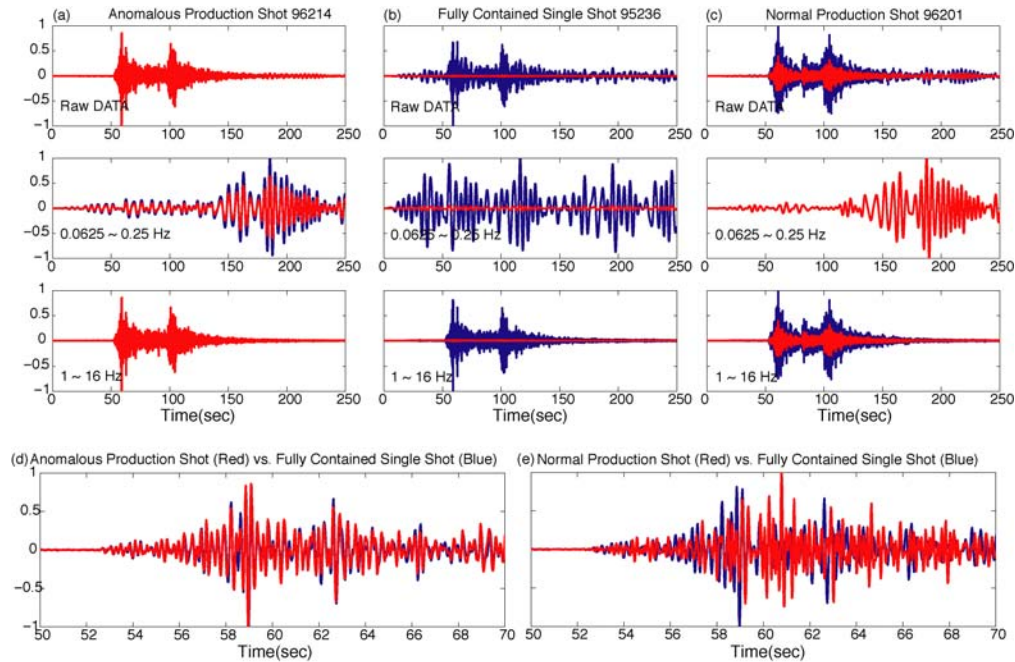


**Figure 3. Spectral composition (raw data and band-pass filtered with bandwidth 0.0625 ~ 0.25Hz; 1 ~ 16Hz) of event 96214 – anomaly (a), event 95236 – single-fired (b), event 96201 – normal (c) recorded at PD31. In each sub-panel, the seismogram in blue is normalized by the maximal amplitude of each event and the red seismogram is normalized by the maximal amplitudes of the three events in the same frequency band; (d) compares 20 s of filtered P wave data (1 ~ 16 Hz) for event 96214 – anomaly (red) and event 95236 – single-fired (blue); and (e) for event 96201 – normal (red) and event 95236 (blue).**

### Seismograms Modeling

Fundamental mode, intermediate period Rayleigh waves generated by the five mining explosions are utilized to constrain the crustal structure of Wyoming (Zhou and Stump, 2004) and NE China (Zhou, 2004). Group velocities of fundamental mode Rayleigh waves were estimated using the Multiple Filter Analysis technique and refined with Phase Matched Filtering. A least square inversion technique was used to invert group velocity dispersion curves for the shallow shear-wave velocity structure. The 1-D structure model along the path to KRET and BJT is presented in Figure 4.

The 96201 blast in Wyoming consisted of 7 rows and 620 decked shots with a total yield of 2,065,412 kg, the largest explosion of those documented in 1996. The inter-shot delay was 35 ms and the inter-row delays ranged from 200 to 275 ms. Multiple charges were detonated in the same hole with different times in a decked charge. In this event, each hole contained two charges separated by 50 to 200 ms. Although the number of shots in each row varied from 85 to 93, for simplicity we assumed each row had 89 shots. The synthetic seismograms were calculated using MineSeis (Yang, 1998). The algorithm assumes the linear superposition of signals from identical single-shot sources composed of isotropic and spall components. Both shooting delays and location differences among individual shots are taken into account in calculating delays of superposition, although the Green's function is assumed to change slowly so that a common Green's function is used for all the single shots. The reflectivity method has been used to calculate the Green's functions.

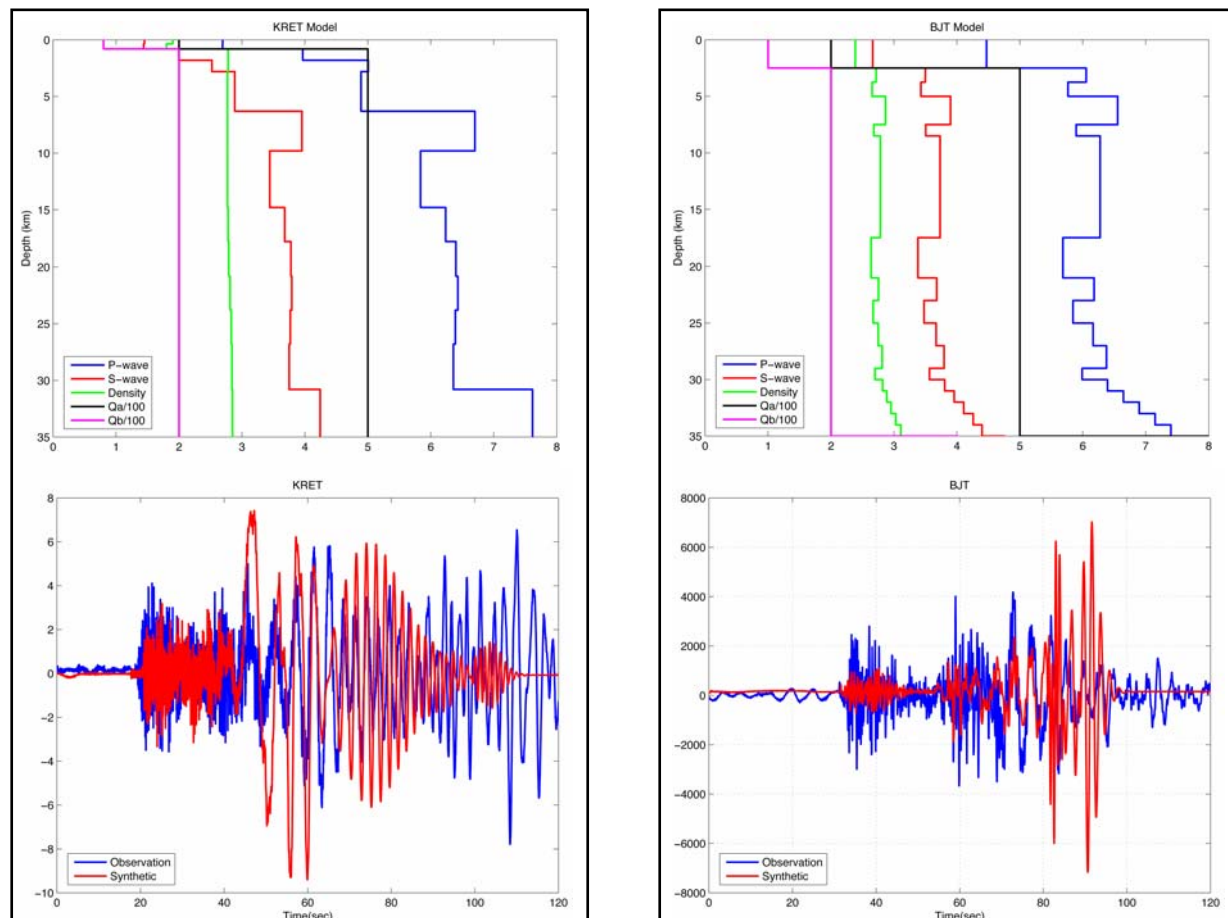


Figure 4. The comparison of synthetic (red) with observational seismograms (blue) at KRET (left) and BJT (right).



The ground truth information for the QianAn explosion is somewhat more limited. The explosion used a total of 1.3 kilotons of explosives designed to move a volume of rock 450 x 150 x 100 m. The source was constructed of 21 individual explosions detonated over 1.3 s. Since the exact dimensions of the spatial and temporal dimensions of the source were unknown the 21 explosions were equally distributed in space and time for seismogram synthesis.

The synthetic seismograms at KRET and BJT are shown in Figure 4 and compared with the observational seismograms. The arrival times of high frequency body waves and long period surface waves match with the observations. And KRET gives a better fit of the P/Lg ratio than the BJT because we have only limited ground truth information for QianAn event, rather than the detailed designed pattern for Wyoming as described earlier. The synthetics and the observations illustrate the strong contribution of the intermediate surface waves in both Wyoming and China. The synthetic study indicates that the presence of these surface waves is strongly dependent upon the relatively long temporal duration of the source for these of mining explosions.

This comparison between synthetic seismograms and observation illustrates the importance of the detail propagation path and ground truth information, the data interpretation, and source characterization.

## DATA

### Yanqing-Huailai Basin Area

Within the Yanqing-Huailai Basin and surrounding area (Figure 5), earthquake risk and propagation path assessments are important because of the historical seismicity and the large population in Beijing and other big cities in this region. Numerous underground mines here regularly experience rock bursts and collapses resulting in the disruption of mining operations, injury, and occasionally death. An understanding of these man made events can lead to a mitigation of these effects as well.

Historically, two large earthquakes occurred in Yanqing-Huailai area. One was the Huailai earthquake with  $M_s$  6.5 on September 8, 1337; the other one was the Shacheng earthquake with  $M_s$  6.75, near Shacheng on July 12, 1720 (open circles in Figure 5). On July 20, 1995, a  $M_L$  4.1 earthquake occurred in the Yanqing-Huailai Basin (white dot in Figure 5) followed by approximately 450 aftershocks (Chen et al., 1998).

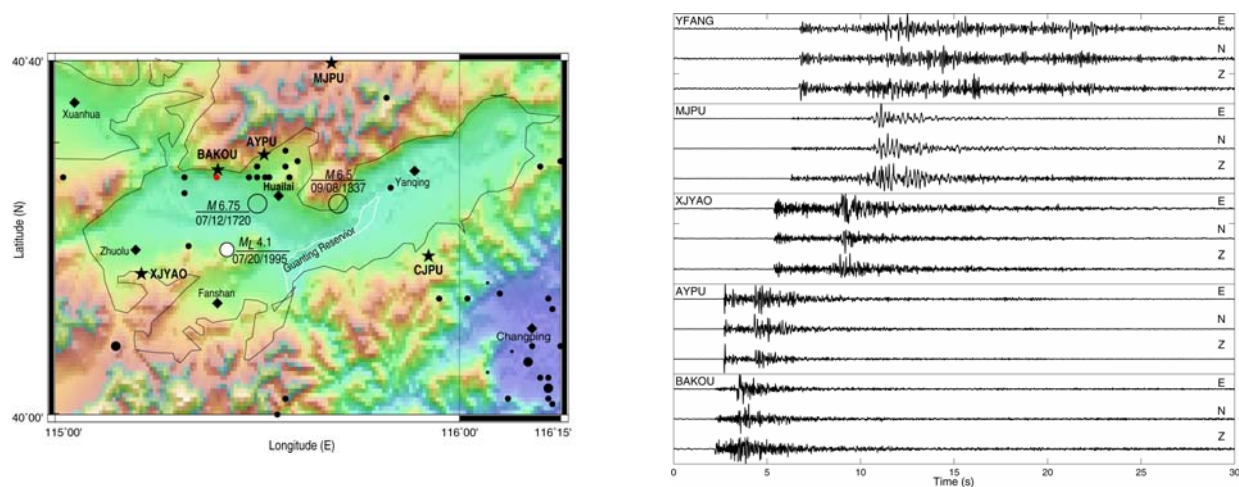


**Figure 5. Left: Seismicity map (solid circles) of Yanqing-Huailai Basin. Stations of the SMU-IGCEA Huailai Seismic Network are designated as stars. Open circles are locations of two historical earthquakes in 1337 and 1720. The white dot is the epicenter of a  $M_L$  4.1 earthquake on July 20, 1995. Diamonds are towns in the area. Right: Seismograms of the Huailai  $M_L$  1.4 earthquake on January 2, 2003 (the epicenter location is a red dot in left figure).**

Man-induced earthquakes occur approximately once a day and include both mining blasts and underground collapses and rock bursts inside the basin (Zhou et. al., 2003). Signals recorded by the SMU-IGCEA Network from events within a few kilometers of the stations often result in repeated signals the analysis of which will help understanding the source and local propagation path characteristics over a broad frequency range.

According to the report from the Hebei Seismic Information Network (<http://www.eq-he.ac.cn>), a magnitude  $M_L$  1.4 earthquake occurred at 40.45°N, 115.4°E on January 2, 2003 (red dot in the left panel of Figure 5). The right panel of Figure 5 shows records of the three components (East: E; North: N and Vertical: Z) of this event at five stations; the records clearly show the good signal-to-noise ratio at all stations. The waveform differences between paths reflect the local geological settings. The short period (1-2 s) surface waves indicate the shallow epicentral depth (5km).

### Haicheng Area

The 1975 Haicheng Earthquake, the first predicted in China, occurred in this region and motivates an interest to understand seismicity for hazard reduction. The Haicheng area is also rich in natural resources such as iron, lead, zinc, coal, oil and natural gas. Mining activities related to resource recovery provide additional sources of seismic waves.

Following the Haicheng network installation, two local events occurred approximately 165 km southwest of the network with magnitude  $M_L$  2.8 (UTC 13:11:0.67) and 3.3 (UTC 13:19:9.6) on August 25, 2004. Four of the five new stations recorded these two events (MJD experienced a power failure). Figure 6 presents the seismograms for these two events at four stations. These data illustrate the value of low noise sites in conducting regional studies of moderate sized events.

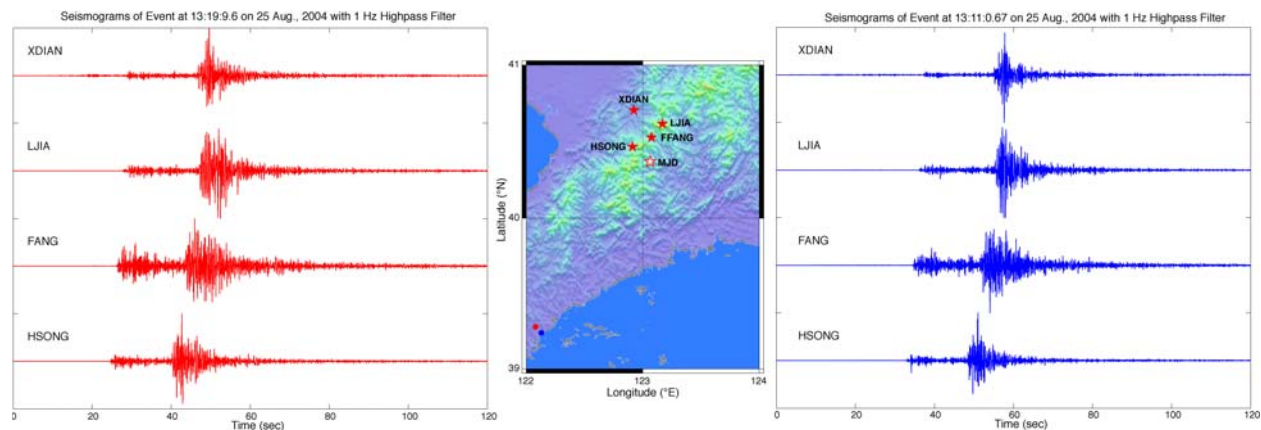


**Figure 6.** Map of the stations (red stars) and epicenters of two local events (dots) on August 25, 2004 with the seismograms (left:  $M_L$  2.8 red dot; and right:  $M_L$  3.3, blue dot).

### CONCLUSIONS AND RECOMMENDATIONS

An important component of this study is the development of detailed source information for selected events, e.g., the QianAn explosion. In this case, detailed data on the location, amount of explosives, and detonation information were provided and used in the modeling and analysis of this unique event (Zhou et al., 2004). We propose to develop similar information for additional events with the cooperation of IGCEA.

Additional ground truth will be acquired for events that occur within or near the two focus areas of our current deployment, Huailai-Yanqing Basin and Haicheng Area. Five broadband stations are closely spaced in each of these areas of significant earthquake activity. These near-source observations can be used to provide source locations of GT10 or GT5 quality as well as source characterization to high frequencies unaffected by regional attenuation. This characterization can then be used to assess propagation path effects to the remaining regional stations.

In the currently deployed regional network, stations are self-contained with local data storage. Because the SMU-IGCEA network is in two widely separated areas (Huailai-Yanqing Basin and Haicheng) and some stations require substantial travel time, it is difficult and expensive to make frequent visits to retrieve data. During the winter it is impossible to visit some of the remote stations. This inability to retrieve frequent data updates has led to data recovery problems since a broken station is not detected for several months. It imposes a substantial load on the analysts, since data arrives in batches of many Gigabytes and substantially lengthens the time required to repair problems, since the instrument turnaround time is so long. The delay in data also makes it difficult to collect ancillary data including news reports and regional seismic data and non-detected segments that may be unarchived. We propose to add real-time telemetry to selected stations to alleviate a number of these problems.

Stump et al. (2004) suggest that the addition of an infrasound array to existing seismic stations can provide additional constraints for source characterization. The addition of infrasound sensors to an existing site can be accomplished for a small incremental installation and operation cost. The combined analysis of seismic and infrasound signals can provide unique constraints on sources near the solid earth – atmosphere boundary (Stump et al., 2004). A variety of man induced and natural events will add to our understanding not only of the source but also the effects of atmospheric propagation as well. We will integrate the seismo-acoustic observations with data from three new proposed infrasound upgrades in China in order to facilitate these source and propagation path studies.

### **ACKNOWLEDGEMENTS**

Equipment for the study was supplied by the PASSCAL Instrumentation Center. We would like to thank Xiang-wei Xu, Shi-yu Bai, and Xiang-tong Xu at the Institute of Geophysics, China Earthquakes Administration, and Mary Templeton at Incorporated Research Institutions for Seismology (IRIS/PASSCAL) Instrument Center for their help with network installation and data collection.

### **REFERENCES**

- Bonner, J. L., D. G. Harkrider, E. T. Herrin, R. H. Shumway, S. A. Russell, and I. M. Tibuleac (2003), Evaluation of short-period, near-regional  $M_s$  scale for the Nevada Test Site, *Bull. Seism. Soc. Am.* 93: 1773–1791.
- Chen, Y.-T., X.-T. Xu, X.-W. Yu and P.-D. Wang (1998). Observations and interpretation of seismic ground motion and earthquake hazard mitigation in Beijing area, *South China Journal of Seismology* 18: 2–8 (in Chinese).
- Denny, M.D., S.R. Taylor, and E.S. Vergino (1987). Investigation of mb and  $M_s$  formulas for the Western United States and their impact on the  $M_s$ /mb discriminant, *Bull. Seism. Soc. Am.* 77: 987–995.
- Evernden, J. F. (1967), Magnitude determination at regional and near-regional distances in the United States, *Bull. Seism. Soc. Am.* 57: 591–639.
- Gutenberg, B. (1945), Amplitudes of surface waves and magnitudes of shallow earthquakes, *Bull. Seism. Soc. Am.* 35: 3–12.
- Marshall, P. D. and P. W. Basham (1972), Discrimination between earthquakes and underground explosions employing an improved  $M_s$  scale, *Geophys. J. R. Astr. Soc.* 28: 431–458.
- Stevens, J. L. and S. M. Day (1985), The physical basis of  $m_b$ : $M_s$  and variable frequency magnitude methods for earthquake/explosion discrimination, *J. Geophys. Res.* 90: 3009–3020.
- Stump, B. W., D. C. Pearson and V. Hsu (2003), Source scaling of contained chemical explosions as constrained by regional seismograms, *Bull. Seism. Soc. Am.* 93: 1212–1225.
- Stump, B., M.-S. Jun, C. Hayward, J.-S. Jeon, I.-Y. Che, K. Thomason, S. House and J. McKenna, 2004, SMALL APERTURE SEISMO-ACOUSTIC ARRAYS: *Design, Implementation and Utilization*, *Bull. Seismo. Soc. Am.* 94: 220–236.



## 27th Seismic Research Review: Ground-Based Nuclear Explosion Monitoring Technologies

- Zhou, R.-M., B. W. Stump, Y.-T. Chen, C. Hayward, Z.-X. Yang, M. Templeton, X.-W. Yu, S.-Y. Bai and X.-T. Xu (2003). Network installation in the Yanqing-Huailai Basin and preliminary study of natural and man-induced events. *Proceedings of the 25<sup>th</sup> Seismic Research Review — Nuclear Explosion Monitoring: Building the Knowledge Base*, LA-UR-03-6029, Vol. 2, pp. 504–513.
- Zhou, R.-M. and B. W. Stump (2004). Rayleigh Waves Generated by Mining Explosions and Upper Crustal Structure Around the Powder River Basin, Wyoming. *Bull. Seismo. Soc. Am.* **94**: 1410–1429.
- Zhou, R.-M., B. W. Stump and C. T. Hayward (2004).  $M_s$ : $m_b$  discrimination study of mining explosions in Wyoming, USA and Qianan, China. *Proceedings of the 26<sup>th</sup> Seismic Research Review: Trends in Nuclear Explosion Monitoring*, LA-UR-04-5801, Vol. 1, pp. 541–550.
- Zhou, R.-M. (2004). Intermediate period surface waves from mining explosions for crustal structure and source studies: application in the Western USA and Northeast China. *Ph. D. Dissertation*, Southern Methodist University, pp 240.
- Yang, X.-N. (1998). MineSeis – A Matlab GUI program to Calculate Synthetic Seismograms from a Linear, Multi-Shot Blast Source Model, *Proceedings of the 20<sup>th</sup> Annual Seismic Research Symposium on Monitoring a Comprehensive Test Ban Treaty*, September, 1998, LA-UR-98-1486, 755–764.